Three-dimensional laser micro-sculpturing of silicone: towards bio-compatible scaffolds

Sima Rekštytė,[1,2] **Mangirdas Malinauskas,**[1,*] **Saulius Juodkazis**[3,4,5]

[1] *Laser Research Center, Department of Quantum Electronics, Physics Faculty,Vilnius University, Saulėtekio Ave. 10, LT-10223 Vilnius, Lithuania*

[2] *Institute of Electronic Structure & Laser, Foundation for Research and Technology - Hellas, Vassilika Vouton, N. Plastira 100, P.O.Box 1527, GR-71110 Heraklion, Greece*

[3] *Centre for Micro-Photonics, Faculty of Engineering and Industrial Sciences Swinburne University of Technology, Hawthorn, VIC, 3122, Australia*

[4] *The Australian National Fabrication Facility - ANFF, Victoria node, Faculty of Engineering and Industrial Sciences, Swinburne University of Technology, Hawthorn, VIC, 3122, Australia*

[5] *Department of Semiconductor Physics, Vilnius University, Saulėtekio 10, Vilnius, LT-10223, Lithuania*

[*] *mangirdas.malinauskas@ff.vu.lt*

Abstract: Possibility to form three-dimensional (3D) micro-structures in silicone elastomer (polydimethylsiloxane; PDMS) doped with different photo-initiators was systematically investigated using direct laser writing with femtosecond laser pulses at different exposure conditions. Accuracy of the 3D structuring with resolution of $\sim 5\ \mu$m and a fabrication throughput of $\sim 720\ \mu m^3$/s, which is exceeding the previously reported values by $\sim 300^{\times}$, was achieved. Practical recording velocities of ~ 1 mm/s were used in PDMS with isopropyl-9H-thioxanthen-9-one (ISO) and thioxanthen-9-one (THIO) photo-initiators which both have absorption at around 360 nm wavelength. The 3D laser fabrication in PDMS without any photo-initiator resulting in a fully bio-compatible material has been achieved for the first time. Rates of multi-photon absorption and avalanche for the structuring of silicone are revealed: the two-photon absorption is seeding the avalanche of a radical generation for subsequent cross-linking. Direct writing enables a maskless manufacturing of molds for soft-lithography and 3D components for microfluidics as well as scaffolds for grafts in biomedical applications.

OCIS codes: (140.3390) Laser materials processing; (220.4000) Microstructure fabrication; (350.3850) Materials processing; (160.1245) Artificially engineered materials.

References and links

1. J. Lotters, W. Olthuis, P. Veltink, and P. Bergveld, "The mechanical properties of the rubber elastic polymer polydimethylsiloxane for sensor applications," J. Micromech. Microeng. **7**, 145–147 (2006).
2. J. Lee, X. Jiang, D. Ryan, and G. Whitesides, "Compatibility of mammalian cells on surfaces of poly(dimethylsiloxane)," Langmuir **20**, 11684–11691 (2004).
3. T. Thorsen, S. Maerkl, and S. Quake, "Microfluidic large scale integration," Science **298**, 580–584 (2002).
4. E. Leclerc, Y. Sakai, and T. Fujii, "Cell culture in 3-dimensional microfluidic structure of PDMS (polydimethylsiloxane)," Biomed. Microdev. **5**, 109–114 (2003).
5. N.-T. Nguyen, "Micro-optofluidic lenses: a review," Biomicrofluidics **4**, 031501 (2010).
6. A. Werber and H. Zappe, "Tunable microfluidic microlenses," Appl. Opt. **44**, 3238–3245 (2005).

#187315 - $15.00 USD Received 18 Mar 2013; revised 24 May 2013; accepted 30 May 2013; published 10 Jul 2013

7. J.-H. Jang, C. Ullal, T. Gorishnyy, V. Tsukruk, and E.L.Thomas, "Mechanically tunable three-dimensional elastomeric network/air structures via interference lithography," Nano Lett. **6**, 740–743 (2006).
8. B. Gates, Q. Xu, J. Love, D. Wolfe, and G. Whitesides, "Unconventional nanofabrication," Annu. Rev. Mater. Res. **34**, 339–372 (2004).
9. C. Coenjarts and C. Ober, "Two-photon three-dimensional microfabrication of poly(dimethylsiloxane) elastomers," Chem. Mater. **16**, 5556–5558 (2004).
10. T. Hasegawa, K. Oishi, and S. Maruo, "Three-dimensional microstructuring of PDMS by two-photon microstereolithography," IEEE **06**, 158–161 (2006).
11. H. Selvaraj, B. Tan, and K. Venkatakrishnan, "Maskless direct micro-structuring of pdms by femtosecond laser localized rapid curing," J. Micromech. Microeng. **21**, 075018 (2011).
12. P. Danilevicius, S. Rekstyte, E. Balciunas, A. Kraniauskas, R. Jarasiene, R. Sirmenis, D. Baltriukiene, V. Bukelskiene, R. Gadonas, and M. Malinauskas, "Micro-structured polymer scaffolds fabricated by direct laser writing for tissue engineering," J. Biomed. Optics **17**, 081405 (2012).
13. M. Malinauskas, A. Zukauskas, V. Purlys, K. Belazaras, A. Momot, D. Paipulas, R. Gadonas, A. Piskarskas, H. Gilbergs, A. Gaidukeviciute, I. Sakellari, M. Farsari, and S. Juodkazis, "Femtosecond laser polymerization of hybrid/integrated micro-optical elements and their characterization," J. Opt. **12**, 124010 (2010).
14. A. Ovsianikov, M. Malinauskas, S. Schlie, B. Chichkov, S. Gittard, R. Narayan, M. Löbler, K. Sternberg, K.-P. Schmitz, and A. Haverich, "Three-dimensional laser micro- and nano-structuring of acrylated poly(ethylene glycol) materials and evaluation of their cytoxicity for tissue engineering applications," Acta Biomater. **7**, 967–974 (2011).
15. S. Turunen, E. Kapyla, K. Terzaki, J. Viitanen, C. Fotakis, M. Kellomaki, and M. Farsari, "Pico- and femtosecond laser-induced crosslinking of protein microstructures: evaluation of processability and bioactivity," Biofabrication p. 045002 (2011).
16. M. Malinauskas, G. Kiršanskė, S. Rekštytė, T. Jonavičius, E. Kaziulionytė, L. Jonušauskas, A. Žukauskas, R. Gadonas, and A. Piskarskas, "Nanophotonic lithography: A versatile tool for manufacturing functional three-dimensional micro-/nano-objects," Lith. J. Phys. **52**, 312–326 (2012).
17. G. von Freymann, A. Ledermann, M. Thiel, I. Staude, S. Essig, K. Busch, and M. Wegener, "Three-dimensional nanostructures for photonics," Adv. Funct. Mater. **20**, 1038–1052 (2010).
18. J. Trull, L. Maigyte, V. Mizeikis, M. Malinauskas, S. Juodkazis, C. Cojocaru, M. Rutkauskas, M. Peckus, V. Sirutkaitis, and K. Staliunas, "Formation of collimated beams behind the woodpile photonic crystal," Phys. Rev. A **84**, 033812 (2011).
19. E. Brasselet, M. Malinauskas, A. Žukauskas, and S. Juodkazis, "Photopolymerized microscopic vortex beam generators: precise delivery of optical orbital angular momentum," Appl. Phys. Let. **97**, 211108 (2010).
20. S. Maruo, K. Ikuta, and H. Korogi, "Force-controllable, optically driven micromachines fabricated by single-step two-photon microstereolithography," J. Microelectromechanic. Syst. **12**, 533–539 (2003).
21. C. Schizas, V. Melissinaki, A. Gaidukeviciute, C. Reinhardt, C. Ohrt, V. Dedoussis, B. Chichkov, C. Fotakis, M. Farsari, and D. Karalekas, "On the design and fabrication by two-photon polymerization of a readily assembled micro-valve," Int. J. Adv. Manuf. Technol. **48**, 435–441 (2010).
22. Y.-L. Zhang, Q.-D. Chen, H. Xia, and H.-B. Sun, "Designable 3D nanofabrication by femtosecond laser direct writing," Nano Today **5**, 435–448 (2010).
23. D. Lipomi, R. Martinez, L. Cademartiri, and G. Whitesides, "Soft lithographic approaches to nanofabrication," Polymer Sci. **7**, 211–231 (2012).
24. C. LaFratta, L. Li, and J. Fourkas, "Soft-lithographic replication of 3d microstructures with closed loops," PNAS **103**, 8589–8594 (2006).
25. P. Danilevicius, S. Rekstyte, E. Balciunas, A. Kraniauskas, R. Sirmenis, D. Baltriukiene, V. Bukelskiene, R. Gadonas, V. Sirvydis, A. Piskarskas, and M. Malinauskas, "Laser 3D micro/nanofabrication of polymers for tissue engineering applications," Opt. Laser Technol. **45**, 518–524 (2013).
26. E. Gamaly, S. Juodkazis, V. Mizeikis, H. Misawa, A. Rode, and W. Krolokowski, "Modification of refractive index by a single fs-pulse confined inside a bulk of a photo-refractive crystal," Phys. Rev. B **81**, 054113 (2010).
27. S. Juodkazis, K. Nishimura, S. Tanaka, H. Misawa, E. E. Gamaly, B. Luther-Davies, L. Hallo, P. Nicolai, and V. Tikhonchuk, "Laser-induced microexplosion confined in the bulk of a sapphire crystal: Evidence of multimegabar pressures," Phys. Rev. Lett. **96**, 166101 (2006).
28. E. E. Gamaly, S. Juodkazis, K. Nishimura, H. Misawa, B. Luther-Davies, L. Hallo, P. Nicolai, and V. Tikhonchuk, "Laser-matter interaction in a bulk of a transparent solid: confined micro-explosion and void formation," Phys. Rev. B **73**, 214101 (2006).
29. M. Malinauskas, V. Purlys, M. Rutkauskas, A. Gaidukevičiutė, and R. Gadonas, "Femtosecond visible light induced two-photon photopolymerization for 3D micro/nanostructuring in photoresists and photopolymers," Lith. J. Phys. **50**, 201–208 (2010).
30. F. Claeyssens, E. A. Hasan, A. Gaidukevičiūtė, D. S. Achilleos, A. Ranella, C. Reinhardt, A. Ovsianikov, X. Shizhou, C. Fotakis, M. Vamvakaki, B. N. Chichkov, and M. Farsari, "Production of biodegradable tissue engineering scaffold materials via 2-photon polymerisation," Langmuir **25**, 3219–3223 (2009).
31. 3DPoli@gmail.com.

#187315 - $15.00 USD Received 18 Mar 2013; revised 24 May 2013; accepted 30 May 2013; published 10 Jul 2013

32. M. Malinauskas, G. Bičkauskaitė, M. Rutkauskas, D. Paipulas, V. Purlys, and R. Gadonas, "Self-polymerization of nano-fibres and nano-membranes induced by two-photon absorption," Lith. J. Phys. **50**, 135–140 (2010).
33. Y. Li, F. Qi, H. Yang, Q. Gong, X. Dong, and X. Duan, "Nonuniform shrinkage and stretching of plymerized nanostructures fabricated by two-photon photopolymerization," Nanotechnology **19**, 055303 (2008).
34. Y. Li, H. Cui, F. Qi, H. Yang, and Q. Gong, "Uniform suspended nanorods fabricated by bidirectional scanning via two-photon photopolymerization," Nanotechnology **19**, 375304 (2008).
35. K. Takada, D. Wu, Q.-D. Chen, S. Shoji, H. Xia, S. Kawata, and H.-B. Sun, "Size-dependent behaviors of femtosecond laser-prototyped polymer micronanowires," Opt. Lett. **34**, 566–568 (2009).
36. S. Juodkazis, V. Mizeikis, S. Matsuo, K. Ueno, and H. Misawa, "Three-dimensional micro- and nano-structuring of materials by tightly focused laser radiation," Bull. Chem. Soc. Jpn. **81**, 411–448 (2008).
37. S. Juodkazis, V. Mizeikis, K. K. Seet, H. Misawa, and U. G. K. Wegst, "Mechanical properties and tuning of three-dimensional polymeric photonic crystals," Appl. Phys. Lett. **91**, 241904 (2007).
38. S. Juodkazis, Y. Nishi, H. Misawa, V. Mizeikis, O. Schecker, R. Waitz, P. Leiderer, and E. Scheer, "Optical transmission and laser structuring of silicon membranes," Opt. Express **17**, 15308–15317 (2009).
39. M. Malinauskas, A. Žukauskas, G. Bičkauskaitė, R. Gadonas, and S. Juodkazis, "Mechanisms of three-dimensional structuring of photo-polymers by tightly focussed femtosecond laser pulses," Opt. Express **18**, 10209–10221 (2010).
40. M. Malinauskas, P. Danilevicius, and S. Juodkazis, "Three-dimensional micro-/nano-structuring via direct write polymerization with picosecond laser pulses," Opt. Express **19**, 5602–5610 (2011).
41. E. G. Gamaly, *Femtosecond Laser-Matter Interactions: Theory, Experiments and Applications* (Pan Stanford Publishing, USA, 2011).
42. S. Juodkazis, A. V. Rode, E. G. Gamaly, S. Matsuo, and H. Misawa, "Recording and reading of three-dimensional optical memory in glasses," Appl. Phys. B **77**, 361–368 (2003).
43. K. Hatanaka, T. Ida, H. Ono, S.-I. Matsushima, H. Fukumura, S. Juodkazis, and H. Misawa, "Chirp effect in hard X-ray generation from liquid target when irradiated by femtosecond pulses," Opt. Express **16**, 12650–12657 (2008).
44. S. Juodkazis, K. Nishimura, and H. Misawa, "Three-dimensional laser structuring of materials at tight focusing," Chin. Opt. Lett. **5**, S198 – 200 (2007).
45. S. Juodkazis, "Writing 3D patterns of microvessels," Int. J. Nanomed. **2012**, 3701 – 3702 (2012).
46. C. Williams, A. Malika, T. Kima, P. Mansonb, and J. Elisseeffa, "Variable cytocompatibility of six cell lines with photoinitiators used for polymerizing hydrogels and cell encapsulation," Biomaterials **26**, 12111218 (2005).

1. Introduction

Silicone or polydimethylsiloxane (PDMS) is an attractive material in microfluidics, micromechanics and biology for its mechanical elasticity [1] and biocompatibility [2]. It enables encapsulation of fluidic chips [3] as well as viable cells [4], production of mechanically tunable microlenses [5, 6] and flexible scaffolds [7]. For a functional usage of PDMS in compact microdevices it is necessary, first, to precisely structure it, preferably in all three-dimensions. Then, a soft-lithography molding technique can be applied for a planar imprinting of various templates [8] for microfluidics and cell cultures.

It has been demonstrated that PDMS can be laser structured using a direct writing with appropriate photo-initiators [9, 10] and thermo-initiators [11]. However, the achieved throughput for the surface and volume structuring at $\sim 6\ \mu\mathrm{m}^2/\mathrm{s}$ and $\sim 12\ \mu\mathrm{m}^3/\mathrm{s}$, respectively, (estimated from the reported data [9, 10]) are still far too small to meet the requirements for practical applications, especially, for bio-scaffolds, where larger volumes of micro-porous templates are required. Much higher volume throughput $\sim 8.75 \times 10^6\ \mu\mathrm{m}^3/\mathrm{s}$ has been demonstrated in fabrication of 3D polymeric scaffolds out of Ormocore b59 [12] and micro-optical elements in SZ2080 resist [13] where a high optical quality of surfaces is required and a surface-defining laser scan is complimented with a uniform post-development exposure by a UV-lamp. So far, those structuring velocities are not demonstrated in bio-compatible photo-polymers despite the technical capabilities of scanning stages and galvano-scanners [14, 15]. This limitation should be overcome by a precise tuning of the light-matter interaction, by implementing protocols combining the movement of stages and scanners, and design of new photo-polymers.

Recently, advances in the direct laser writing (DLW) employing ultrashort pulses (10 fs to 10 ps) is proving to be an advantageous approach for a precise high resolution fabrication of

#187315 - $15.00 USD Received 18 Mar 2013; revised 24 May 2013; accepted 30 May 2013; published 10 Jul 2013

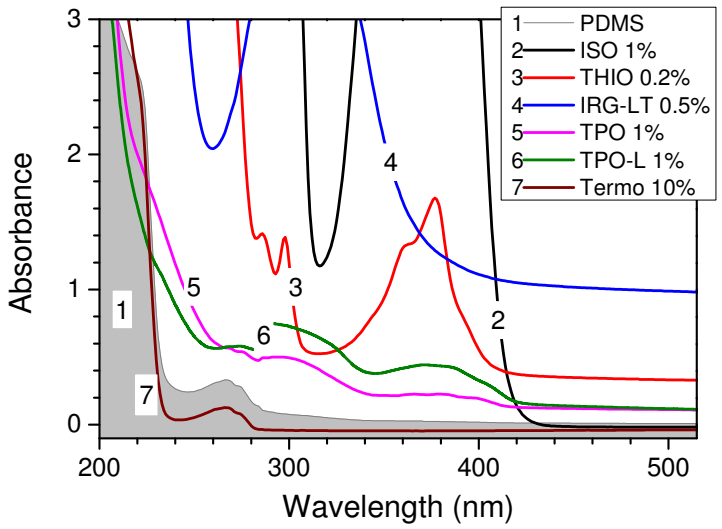

Fig. 1. Absorption spectra of PDMS samples with different photo-initiators (see, Table 1). Absorption spectra are clipped at optical density $OD = 3$ ($Intensity/10^3$-level). Thickness of drop cast photo-polymer was $\sim$1 mm.

2D and 3D structures at an increasing throughput [16]. By employing the interference or direct writing, features down to $\sim$100 nm in spatial resolution can be obtained. Thus the DLW has became an established technique for custom fabrication of structures required in photonics [17, 18], micro-optics [13, 19], microfluidics [20, 21], artificial scaffolds [12, 14], and other fields [22]. PDMS is an attractive material for a soft-lithography molding [23], especially for 3D and large area replication [24, 25].

Here, we systematically studied and optimized a PDMS doping with prospective photo-initiators for the augmented fabrication throughput in terms of *area* and *volume* per *time*. The fabrication throughput was calculated by the following formulas for the 2D and 3D cases, respectively: $V_{2D} = v \times dx$ and $V_{3D} = v \times dx \times dz$, where v is the laser scan velocity, dx is the distance between parallel scans in x- or y-direction (lateral), dz is the distance between parallel scans in z-direction (axial). The exposure parameters of a fs-laser irradiation were tested to reveal the importance of the multi-photon and avalanche ionization at the close-to-the-dielectric-breakdown conditions; the breakdown typically occurs at $7-10$ TW/cm^2 in crystals and glasses under tight focusing [26–28]. We show that a pure PDMS without photo-initiator can be 3D structured by solely tuning the exposure conditions of laser irradiation. A fabrication resolution typical for bio-scaffolds ~ 5 μm was used for benchmarking different photo-initiators (the quest for the highest resolution was beyond the scope of this study).

2. Experimental

2.1. Materials

A commercial elastomeric PDMS kit (Sylgard 184, Dow Corning) was used to prepare samples for the fs-laser structuring. The pre-polymer used for the laser-induced polymerization was made by a two step process: first, photo-initiator was dissolved in a tetrahydrofuran (THF), then, solution was added to the PDMS pre-polymer and left overnight on a magnetic stirrer. For the experiments with laser setup No. 1 (Sec. 2.2), three different photo-initiators were used:

#187315 - $15.00 USD Received 18 Mar 2013; revised 24 May 2013; accepted 30 May 2013; published 10 Jul 2013

namely, thioxanthen-9-one (THIO), isopropyl-9H-thioxanthen-9-one (ISO) and 2-benzyl-2-(dimethylamino)-4'-morpholinobutyrophenone (IRG2). The concentration of THIO in PDMS was 0.2 wt %, ISO – 0.2, 0.5 or 1 wt % and IRG2 – 0.5 wt %. Samples for the laser structuring were prepared by drop-casting on a cover glass substrate and then heating at $\approx 100^{\circ}$C temperature for 30 min to evaporate the THF solvent.

For experiments with the laser setup No. 2 (Sec. 2.2) thirteen different photo-initiators were tested:

1) *2-benzyl-2-dimethylamino-1-(4-morpholinophenyl)-butanone-1 (Irgacure 369)* – IRG1 (Ciba),
2) *4,4'-bis(diethylamino)-benzophenone* – BIS1 (Sigma Aldrich),
3) *isopropyl-9H-thioxanthen-9-one* – ISO (Sigma Aldrich),
4) *lucirin TPO* – TPO (BASF),
5) *lucirin TPO-L* – TPO-L (BASF),
6) *2-hydroxy-4'-(2-hydroxyethoxy)-2-methylpropiophenone* – HYD (Sigma Aldrich),
7) *2-benzyl-2-(dimethylamino)-4'-morpholinobutyrophenone* – BEN (Sigma Aldrich),
8) *phenylbis (2,4,6-trimethylbenzoyl)-phosphine oxide* – PHE (Sigma Aldrich),
9) *(1S)-(+)-camperchinon* – CAM (Sigma Aldrich),
10) *2,2-dimethoxy-2-phenylacetophenone* – DIM (Sigma Aldrich),
11) *2-benzyl-2-(dimethylamino)-4'-morpholinobutyrophenone* – IRG2 (Sigma Aldrich),
12) *4,4'bis(dimethyl-amino)-benzophenon* – BIS2 (Fluka),
13) *thioxanthen-9-one* – THIO (Sigma Aldrich).

Solubility of photo-initiators in the PDMS is summarized in Table 1. The photo-initiators were dissolved, at first, in THF (except the TPO-L which is liquid, and was added to PDMS directly) and only then added to PDMS. Figure 1 shows typical absorption spectra of the samples: resin sandwiched between two cover glasses with the cover glass absorption subtracted.

To avoid heat modification of the samples, the mixture was left stirring overnight at the ambient conditions for the THF evaporation. Then, before the laser fabrication a heating at $\approx 90^{\circ}$C for 30 min was applied for the final removal of solvent. The laser structuring experiments (setup No. 2) were performed with all the mixtures even with the ones in which photo-initiator did not dissolve completely. After laser fabrication, the samples were immersed in a methyl isobutyl ketone for ≈ 30 min to rinse the unexposed resin. Samples were inspected by a scanning electron microscopy (SEM) after applying a 10 nm conductive gold layer by sputtering.

2.2. Laser setup

We used two different fs-laser fabrication systems (see, Fig. 2(a)) which allowed us to explore effects of pulse duration, thermal accumulation and wavelength. A more detailed description of the systems can be found elsewhere [29, 30]. The results are analyzed with a focus on the fabrication throughput and influence of photo-initiator performance rather a detailed comparison of all the used fabrication conditions. Here we list the main parameters setups.

The first setup No. 1 had a fs-laser Pharos (Light Conversion) laser operating at the 1030 nm fundamental wavelength. The second harmonic at 515 nm was used for fabrication with

#187315 - $15.00 USD Received 18 Mar 2013; revised 24 May 2013; accepted 30 May 2013; published 10 Jul 2013

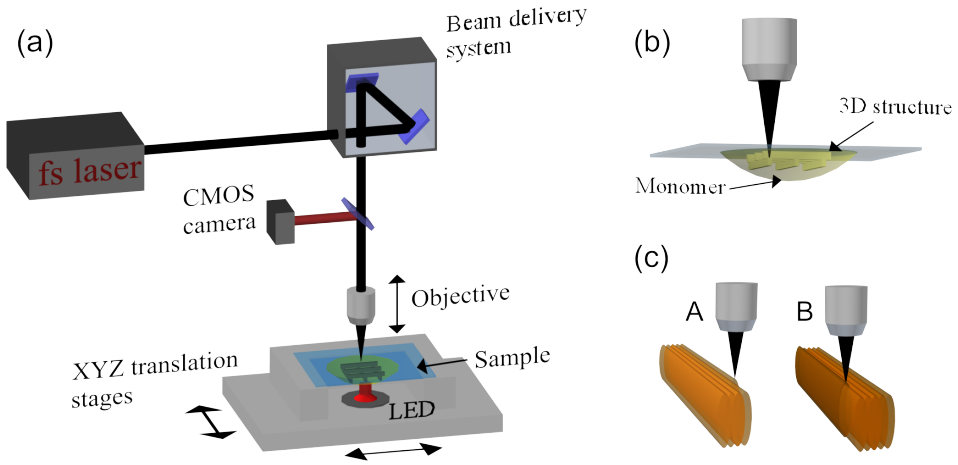

Fig. 2. (a) Fs laser fabrication setup with *in situ* monitoring of fabrication (setups No.1 and 2 (Sec. 2.2) differed in wavelength, pulse duration, and sample scanning). (b) Close-up view of sample: polymerization is performed starting from the substrate's surface, when further layers are being formed as the laser beam is focussed through previously polymerized parts of the structure. (c) Multipath scanning. A – a line is formed by several parallel laser beam scans; B – the line is scanned repeatedly along the same path to strengthen the polymerized region.

300 fs pulses at a 200 kHz repetition rate. The polymerization trajectory was controlled by xy-galvanometric scanners (SCANLAB hurrySCAN II 10) and a sample positioning system Aerotech ALS130-100 (x and y-axis) and ALS130-50 (z-axis) linear motion stages ensuring the positioning resolution of 50 nm. 3DPoli software took control over a laser exposure automation of the sample [31].

The second setup No. 2 had a Ti:Sapphire fs-laser operating at a 800 nm fundamental wavelength delivering 20 fs pulses at a 75 MHz repetition rate. The beam was scanned in x and y-directions by a galvano-mirror digital scanner (SCANLAB hurrySCAN II) controlled with SAMLight (SCAPS) software. A large scale lateral movement as well as the movement along z-axis was handled by step motors (PI Instruments).

In both systems fabrication was monitored in real time using a sample illumination setup consisting of a LED light and a CMOS camera. A cover glass was used as a substrate with pre-polymer pointing downwards. This allowed the use of the immersion oil objectives for laser fabrication. The peak irradiance assuming a Gaussian intensity envelope is $I_p = \frac{T \times 2P_{av}}{f_r t_p S}$ while the average intensity is $I_{av} = I_p/2$. The dielectric breakdown was observed at the peak intensity $I_p \approx 1.44$ TW/cm^2 with setup No. 1 and $I_p \approx 5.42$ TW/cm^2 with setup No. 2 (for PDMS:ISO) and $I_p \approx 1.92$ TW/cm^2 with setup No. 1 (for PDMS:THIO) by *in situ* monitoring at the scanning velocities of 1 mm/s.

3. Results and discussion

The two laser setups No. 1 and 2 have different capabilities in terms of repetition rate (hence, thermal accumulation), also wavelength, and pulse duration. We benchmarked them for the fabrication throughput measure and quality of 2D and 3D structures in PDMS. The role of photo-initiator and the mechanisms of polymerization at the high irradiance were qualitatively compared. The resolution limits were not tested; we fabricated structures with resolution typical

#187315 - $15.00 USD Received 18 Mar 2013; revised 24 May 2013; accepted 30 May 2013; published 10 Jul 2013

for the bio-scaffolds.

3.1. Formation of 3D structures with a 800 nm/20 fs high-repetition exposure

Table 1 summarizes the results of grid pattern fabrication in PDMS doped with different photo-initiators using $\lambda = 800$ nm and $t_p = 20$ fs pulses at a high repetition rate (the laser setup No. 2). Very short pulses minimize thermal accumulation while the high $f_r = 75$ MHz repetition rate allows for a thermal accumulation between subsequent pulses which depends on a scan velocity, v_s. Typically at a 1.5% wt loading of photo-initiator, the resin becomes turbid and this always hampers or renders impossible the 3D structuring. Only a few initiators show promising results and 3D structures can be obtained. PDMS without photo-initiator was not polymerizable with the laser setup No. 2.

Table 1. PDMS structuring with different photo-initiators (PI). Exposure conditions (laser setup No. 2): objective lens $100^{\times}$ magnification, numerical aperture $NA = 1.4$, average power $P_{av} = 53$ mW (before the lens), scan velocity $v_s = 10 - 40$ μm/s at the repetition rate $f_r = 75$ MHz. Overall transmission coefficient through the lens to the exposure point was $T = 0.235$ for the 800 nm wavelength. After the laser fabrication, samples were immersed in a methyl isobutyl ketone for ≈ 30 min to rinse the unexposed resin.

No.	PI	PI conc. [% wt]	Mixture's transparency	Polymerization observed Yes(+) No(-)	Objects survive development Yes(+) No(-)	3D throughput [μm^3/s]
1	IRG1	0.5	not transparent	–	–	
2	BIS1	0.5	not transparent	–	–	
3	ISO	0.5	transparent	+	+	
3-a	ISO	1	transparent	+	+	20
3-b	ISO	1.5	not transparent			
4	TPO	0.5	transparent	+	–	
4-a	TPO	1	transparent	+	–	
4-b	TPO	1.5	not transparent			
5	TPO-L	0.5	transparent	+	–	
5-a	TPO-L	1	transparent	+	–	
5-b	TPO-L	1.5	not transparent			
6	HYD	0.5	not transparent	–	–	
7	BEN	0.5	not transparent	–	–	
8	PHE	0.5	not transparent	–	–	
9	CAM	0.5	transparent	–	–	
10	DIM	0.5	transparent	–	–	
11	IRG2	0.5	transparent	+	+	
12	BIS2	0.2	transparent	+	–	
13	THIO	0.2	transparent	+	+	
14	none	–	transparent	–	–	

A tight focusing with an objective lens of $100^{\times}$ magnification and numerical aperture $NA = 1.4$ (with transmission $T = 0.235$) was used to record the test structures. Before a laser exposure, solubility of all thirteen photo-initiators in PDMS was tested at different concentrations. Samples were exposed to laser radiation using an average power of $P_{av} = 53$ mW; the peak irradiance assuming a Gaussian intensity envelope then is $I_p = \frac{T \times 2P_{av}}{f_r t_p S} \approx 4.35$ TW/cm^2. We checked whether any polymerization can be observed with focusing inside pre-polymer at

#187315 - $15.00 USD Received 18 Mar 2013; revised 24 May 2013; accepted 30 May 2013; published 10 Jul 2013

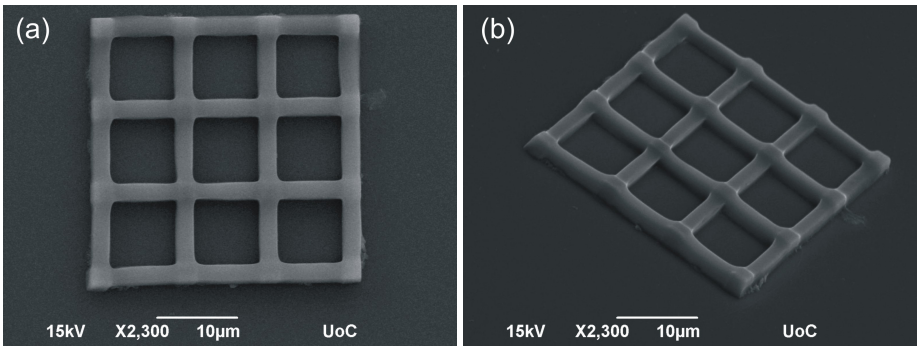

Fig. 3. (a,b) 2D grid fabricated in PDMS with 1% ISO. Exposure conditions: $P_{av} = 64$ mW ($I_p \approx 5.25$ TW/cm^2), $v_s = 150$ μm/s (throughput of 30 μm^2/s); 6 layers in z-axis $dz = 0.5$ μm, 0.2 μm hatching in x and y-axis. Intersections of the grid walls are taller than other areas due to double exposure dose acquired due to overlapping scanning trajectories.

different scanning velocities v_s. Only the mixtures with a visible polymerization were used in the next step: polymerization of simple 2D grids. These mixtures were: PDMS with ISO, TPO, TPO-L, IRG2, BIS2 and THIO (see Table 1).

Then, we investigated if a larger amount of these photo-initiators can be dissolved in PDMS. Up to 1 % of ISO, TPO and TPO-L was dissolved without apparent change of the optical transparency. These mixtures together with those doped with THIO, IRG2 and BIS2 were then investigated using laser powers up to 90 mW ($I_p \approx 7.38$ TW/cm^2) for fabrication of 2D grids; we define structures being 2D if the width of the grid log/beam is comparable with its height, hence the aspect ratio $f_{ar} = height/width \leq 1$ and structure is 3D if $f_{ar} > 1$. The best structuring results were obtained using ISO, although some 2D structures fabricated with THIO and IRG2 also survived the development. However, the quality of THIO and IRG2 structures as well as used velocities (40 μm/s) for their fabrication were not promising for the practical applications. Thus, the ISO doping was chosen for the further investigation.

Grids formed out of PDMS mixed with 1% wt. ISO are shown in Fig. 3. Structures were made of 6 layers staggered axially with separation $\Delta z = 0.5$ μm and hatching in lateral x- and y-directions by $\Delta x = \Delta y = 0.2$ μm at laser power of $P_{av} = 64$ mW ($I_p \approx 5.25$ TW/cm^2) and scanning velocity was $v_s = 150$ μm/s (cumulative dose of the exposure $D_{ac} = E_p \times N_p \approx 18$ kJ/cm^2, where number of pulses over the spot size $2w_0$ is $N_p = 2w_0/(v_s/f_r)$). This very large dose indicates that photo-polymerization is not an efficient process and this is why photo-initiation has to be used.

Next, for fabrication of 3D structures we had to take into account that PDMS:ISO is in a liquid state, hence, polymerization has to start from the glass substrate to anchor the 3D structure (see, Fig. 2(b)). As a result, formation of the 3D pattern is carried out by focusing throughout the already polymerized regions. This introduced beam distortions and change of focusing conditions which have to be addressed. We implemented two solutions: (i) different laser power was used at a different depth and (ii) an increased exposure dose of the far-outer layers by increased number of scans (Fig. 2(c)). Results of the two strategies are shown in Fig. 4. By increasing the exposure dose of the outer (more distant axially) layers 3D structures were retrieved with structure closer to the designed pattern (see, panels (c,d)). The largest 2D and 3D throughput using the laser setup No. 2 were 30 μm^2/s and 20 μm^3/s, respectively.

#187315 - $15.00 USD Received 18 Mar 2013; revised 24 May 2013; accepted 30 May 2013; published 10 Jul 2013

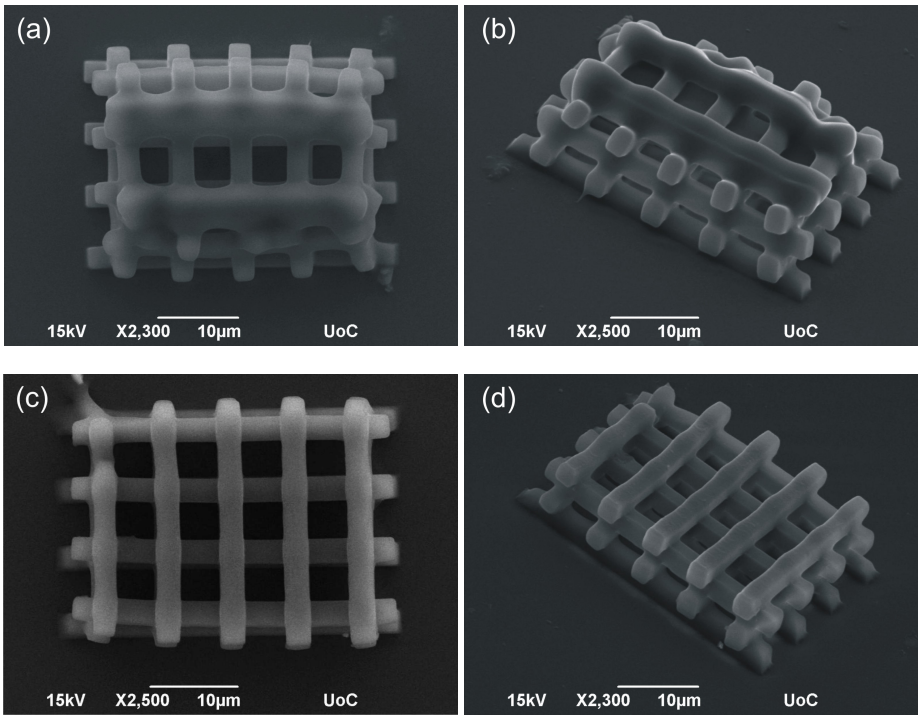

Fig. 4. (a, b) 3D structure fabricated in PDMS:ISO 1%. Parameters used: incremental power $P_{av} = 62 - 64 - 67$ mW ($I_p \approx 5.09 - 5.25 - 5.50$ TW/cm^2), $v_s = 150$ μm/s (throughput of 20 μm^3/s), 30 layers in z-axis $\Delta z = 0.5$ μm, hatching laterally 0.2 μm. (c-d) 3D structure fabricated out of ISO 1%. Parameters used: P_{av} = 64 mW ($I_p \approx 5.25$ TW/cm^2) and second scanning with P_{av} 55 mW ($I_p \approx 4.51$ TW/cm^2) for the last two layers, $v_s = 150$ μm/s (throughput of 15 μm^3/s), 24 layers in z-axis $\Delta z = 0.5$ μm, hatching laterally 0.2 μm.

3.2. Formation of 3D structures with a 515 nm/300 fs sub-1 MHz repetition exposure

With the laser setup No. 1 fully 3D microstructures were fabricated out of PDMS using two different photo-initiators (THIO and ISO) using 100$^\times$ magnification $NA = 1.25$ objective lens (transmission T = 0.14) as well as pure PDMS without photo-initiator. Experiments with different mixtures were performed by fabricating arrays of the same 3D structure changing the laser power and sample translation velocity. At first, only linear stages were used for sample translation. The distance between parallel scans in these structures in x and y-axis were 0.3 μm and the distance between layers in z-axis was 0.4 μm. The resolution of structuring achieved was ≈ 5 μm laterally and ≈ 3 μm axially. It is important to note, that higher resolution is possible to achieve but we used a typical resolution for the bio-scaffold fabrication in this study.

The 3D structures out of PDMS mixed with 0.2% THIO (Fig. 5(a)) were made using sample translation velocity of up to 1 mm/s with P_{av} = 0.68 mW ($I_p \approx 1.63$ TW/cm^2, $D_{ac} \approx 24.63$ J/cm^2) with fabrication throughput of 120 μm^3/s. It can be seen that shape is not recovered with high fidelity as compared to the design. PDMS tends to round off the corners of the structure. Surface tension (or surface energy) of PDMS is 20 mN/m (mJ/m^2) [32–35] and together with cross-linking quality [36] are defining the final shape of the structure. Mechanical strength of the structures depends on the polymer crosslinking and the volume fraction [37]. An achievable resolution also depends on the surface energy of material and cross-linking reaction

#187315 - $15.00 USD Received 18 Mar 2013; revised 24 May 2013; accepted 30 May 2013; published 10 Jul 2013

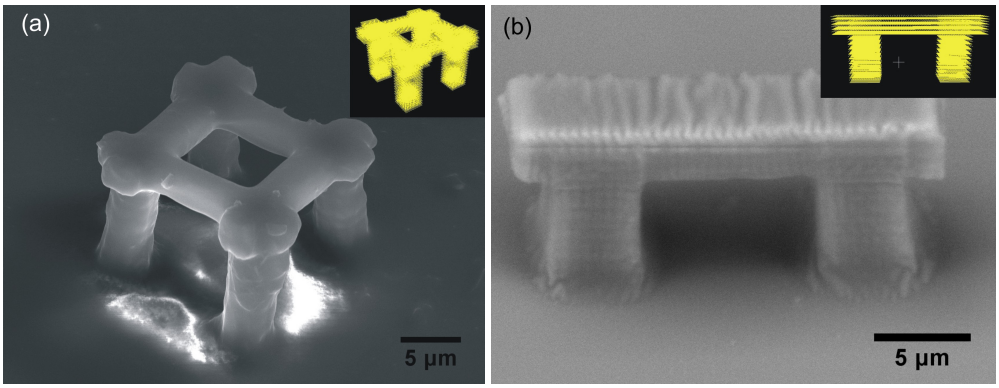

Fig. 5. SEM micrograph of 3D structures fabricated in PDMS. (a) THIO 0.2%. Parameters used: power $P_{av} = 0.8$ mW ($I_p \approx 1.92$ TW/cm^2), $v_s = 150$ μm/s, $\Delta z = 0.4$ μm, hatching 0.3 μm. (b) ISO 0.5%. Parameters used: power $P_{av} = 0.7$ mW ($I_p \approx 1.68$ TW/cm^2), $v_s = 4$ mm/s, $\Delta z = 0.4$ μm, hatching 0.3 μm. The designed models are shown in the insets.

whose rate, α, scales as $d\alpha/dt = A\exp(-E_a/(RT))(1-\alpha)^n$, where E_a is the activation energy, T is the temperature, R is the gas constant, and n is the order parameter. Surface tension tends to round the sharp corners and this effect is even more exacerbated for the weaker cross-linked regions (see, Fig. 4). Mechanisms relevant to polymerization are discussed next in Sec. 3.3.

Experiments were also performed using PDMS mixed with various quantities of ISO photo-initiator (0.2, 0.5 and 1% wt). Good quality 3D structures were made out of PDMS mixed with 0.2% and 0.5% wt ISO (Fig. 5(b)). Using 0.5% wt ISO sample translation velocity of up to 1.5 mm/s was achieved (P_{av} = 0.5 mW, $I_p \approx 1.20$ TW/cm^2, $D_{ac} \approx 12.07$ J/cm^2) giving fabrication throughput of 180 μm^3/s.

PDMS mixed with IRG2 was also used for laser structuring using multi-path scanning (which is proven to be the best for 3D structures as discussed above) with velocities of up to 30 μm/s and focusing with a dry 40$^\times$ magnification $NA = 0.65$ objective lens. The acquired throughput of 2D structures was ≈ 10 μm^2/s.

Pure PDMS without a photo-initiator can be 3D polymerized using translation velocity of up to 1 mm/s with P_{av} = 0.7 mW ($I_p \approx 1.68$ TW/cm^2, $D_{ac} \approx 25.36$ J/cm^2) giving a fabrication throughput of 120 μm^3/s as shown in Fig. 6. PDMS structuring results using laser setup No. 1 are summarized in Table 2.

It was noticed that using the same fabrication parameters the quality of the structures was considerably worse when only the stages were used for sample translation as compared to the structures fabricated using stages combined with galvano-scanners (see, Fig. 7). Higher fabrication throughput was also achieved in the later case ($v_s = 1.5$ mm/s, throughput of 180 μm^3/s with pure PDMS and 0.2% wt THIO, and $v_s = 6$ mm/s, throughput of 720 μm^3/s with 0.5% wt ISO).

It is noteworthy, the use of second harmonics makes perfect cancellation of the nanoseconds long pedestal of the fs-laser pulse which can affect ionization at the focus [38]. Also, the wavelength $\lambda = 515$ nm is perfectly matching the two photon absorption conditions of the THIO and ISO which have direct absorption peak at approximately 360 nm $= 0.7 \times \lambda$ (see, Fig. 1) [39]. The largest 2D and 3D throughput using the laser setup No. 1 were 1800 μm^2/s and 720 μm^3/s, respectively.

#187315 - $15.00 USD Received 18 Mar 2013; revised 24 May 2013; accepted 30 May 2013; published 10 Jul 2013

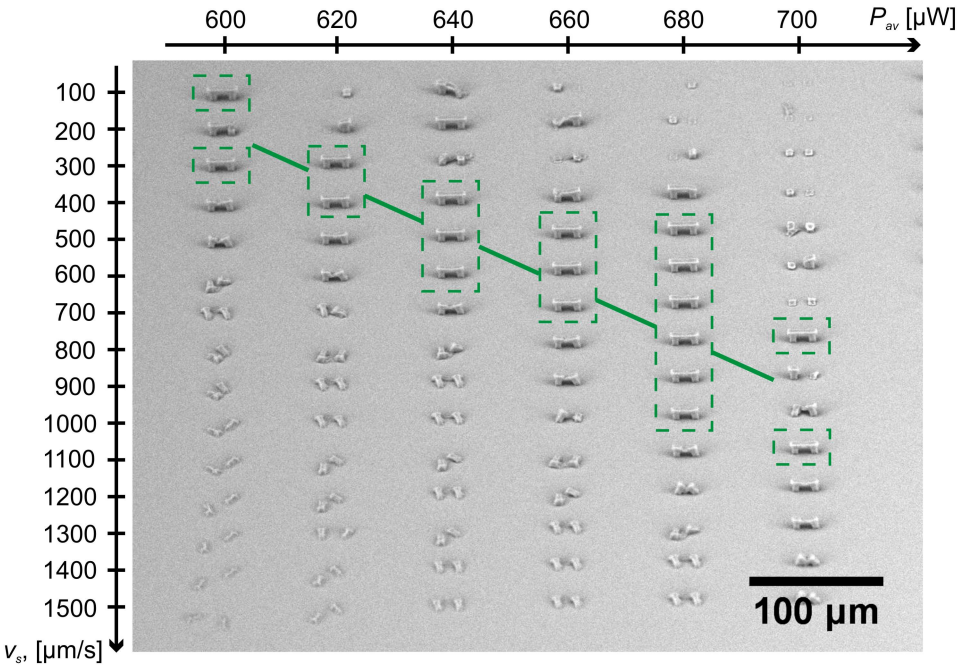

Fig. 6. SEM micrograph of an array of 3D structures fabricated out of pure PDMS. The cumulative energy $E_{ac} = \frac{E_p}{v_s}(2w_0 f_r) \propto \frac{P_{av}}{v_s}$ scales linearly with an average power $P_{av} = E_p f_r$. The best fabrication conditions (a fidelity of recovered 3D structures) scales linearly in presentation P_{av} *vs*. v_s (this is more clearly appreciated in a log - log presentation) indicating a linear process of polymerization. Dashed lines mark good quality structures.

Table 2. PDMS structuring with different photo-initiators using laser setup No. 1 ($\lambda = 515$ nm, $t_p = 300$ fs, $f_r = 200$ kHz). PI numbering is kept from Table 1 with addition of 3-c corresponding to 0.2 % concentration of ISO which was not used previously.

No.	PI	PI conc. [% wt]	Mixture's transparency	Polymerization observed Yes(+) No(-)	Objects survive development Yes(+) No(-)	3D throughput [μm^3/s]
3-c	ISO	0.2	transparent	+	+	
3	ISO	0.5	transparent	+	+	720
3-a	ISO	1	transparent	+	+	
11	IRG2	0.5	transparent	+	+	
13	THIO	0.2	transparent	+	+	180
14	none	–	transparent	+ (Isttime)	+ (Ist time)	180

3.3. Mechanisms of polymerization

In practical applications very different laser fabrication conditions are used: wavelength, λ, pulse duration, τ_p, repetition rate, f_r, peak irradiance, I_p (which is important for the nonlinear absorption and refraction), and the exposure dose or a number of overlapping pulses, N_p. We present here generic estimations of electron generation rates, hence, bond breaking proba-

#187315 - $15.00 USD Received 18 Mar 2013; revised 24 May 2013; accepted 30 May 2013; published 10 Jul 2013

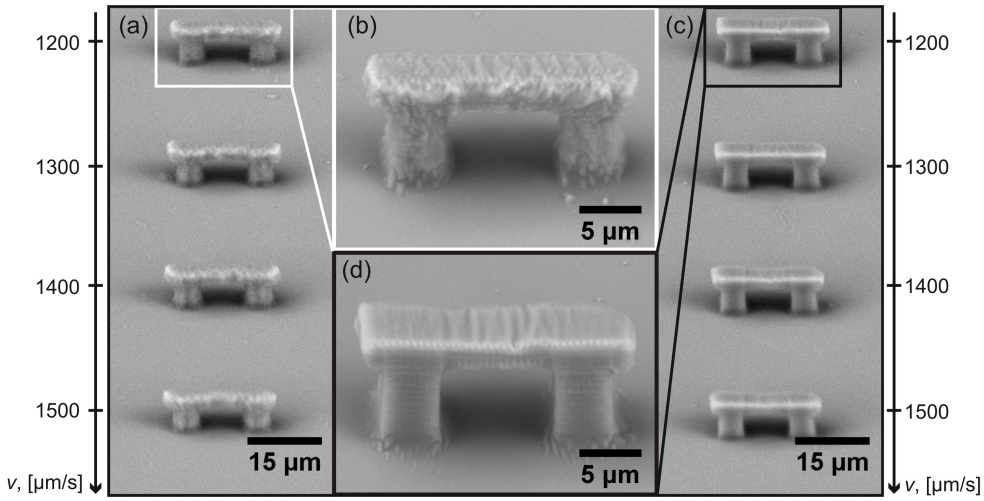

Fig. 7. (a – b) 3D structures fabricated using only linear translation stages for sample translation; (c – d) using stages combined with galvanometric scanners. (b) and (d) show magnified images of the structures, fabricated using the same parameters ($P_{av} = 0.5$ mW, $I_p \approx 1.20$ TW/cm^2, $v_s = 1.2$ mm/s.)

bility which facilitates a polymer cross linking. These order of magnitude estimations predict qualitatively well the thresholds of dielectric breakdown of SZ2080 resist with different photo-initiators and explain the mechanism of polymerization using fs- and ps-laser pulses [39, 40].

The multi-photon absorption and avalanche rates of electron multiplication w_{mpi} and w_{imp}, respectively, are given by [41]:

$$w_{mpi} \simeq w n_{ph}^{3/2} \left(\frac{\varepsilon_{osc}}{2J_i} \right)^{n_{ph}}, \tag{1}$$

$$w_{imp} \simeq \frac{\varepsilon_{osc}}{J_i} \frac{2\omega^2 \nu_{e-ph}}{\left(\nu_{e-ph}^2 + \omega^2 \right)}, \tag{2}$$

where $n_p h = J_i e/(h\omega) + 1$ is the number of photons required for direct absorption (truncated to an integer) with J_i being the ionization potential of material, h Plank's constant, $\omega = 2\pi c/\lambda$ is the cyclic frequency of light of wavelength λ, e electron charge, and c speed of light. The electron quiver energy $\varepsilon_{osc} = \frac{e^2 E^2}{4m\omega^2}$ with the electrical field strength defined by intensity/irradiance, I_p, as $E = \sqrt{I_p/(c\varepsilon_0 n)}$, where ε_0 is the vacuum permittivity constant and n is the refractive index of the ambience (material). The electron ion interaction is governed by the electron-phonon momentum exchange rate, ν_{e-ph}.

With the multi-photon absorption and avalanche rates estimated by Eqns. 1 and 2, it is possible to calculate the rate of free electron generation, hence, the rate of free radical creation:

$$\frac{dn_e}{dt} = n_e w_{imp} + n_a w_{mpi}, \tag{3}$$

where n_e is free electron density (available only for the avalanche multiplication) and n_a is the atom density (available only for the multi-photon ionization). Solution of Eqn. 3 is following:

$$n_e(I, \lambda, t) = \left[n_{e0} + \frac{n_a w_{mpi}}{w_{imp}} [1 - e^{-w_{imp} t}] \right] e^{w_{imp} t} \tag{4}$$

#187315 - $15.00 USD Received 18 Mar 2013; revised 24 May 2013; accepted 30 May 2013; published 10 Jul 2013

This equation allows to explicitly follow the ionization in time $I(t)$ [42]; here n_{e0} is the initial (dark) electron density in material $\sim 10^{10}$ cm^{-3}.

Let us evaluate the values of w_{mpi} and w_{imp} for the used polymerization of undoped PDMS which has a strong absorption at $\lambda_g \simeq 225$ nm or $J_i = 5.5$ eV (see, Fig. 1) considered here as the direct absorption transition. Then a 3-photon process is required $n_{ph} = 3$ at the laser fabrication wavelength $\lambda = 515$ nm for the free electron generation. For the typical pulse intensity $I_p = 2.5$ TW/cm^2 used in 2/3D fabrication: $w_{mpi} = 1.5 \times 10^8$ s^{-1} and $w_{imp} = 4.7 \times 10^{12}$ s^{-1}, respectively, for the focusing inside PDMS; the refractive index $n = 1.4 - 1.42$ (according to the manufacturer) and electron quiver energy $\varepsilon_{osc} = 4$ meV. The value $\nu_{e-ph} \simeq 6 \times 10^{14}$ s^{-1} [39] was not critically important for the estimation of mechanisms discussed here. Obviously, in the undoped PDMS $w_{imp} \gg w_{mpi}$ and this explains that sometimes a strong optical damage occurred during polymerization and a very high irradiance was required. If only a seeding of free electrons is provided from defect states and/or impurities in PDMS matrix, a strong avalanche makes a run away breakdown (see Table 1).

In the case of PDMS with ISO and THIO the absorption band exist at $\lambda_g = 375$ nm, $J_i = 3.3$ eV (see, Fig. 1). For the same $I_p = 2.5$ TW/cm^2, one would find $w_{mpi} = 1.2 \times 10^{11}$ s^{-1} and $w_{imp} = 7.8 \times 10^{12}$ s^{-1} which are the rates on ionization of the photo-initiator molecules. Now, only $n_{ph} = 2$ is required for ionization of ISO and THIO and the two-photon absorption rate is only slightly smaller than the avalanche. The doping efficiently provides seeding electrons for ionization of the rest of PDMS matrix and allows to control overall ionization and free radical generation rate.

The estimations presented above are based on the peak intensity $I_p = E_p/\tau_p$ per pulse and the same values for $\tau_p = 300$ fs (setup No. 1) and $\tau_p = 20$ fs (setup No. 2) can be achieved at proportionally different pulse energies, E_p. Small E_p is beneficial for a precise control of the energy delivery and reduces chances of a run away breakdown. At the high repetition rate $f_r > 1$ MHz, a thermal accumulation is important as we recently demonstrated [40]. The number of pulses overlapped per focal spot $N_p = 2w_0/(v_s/f_r)$ in the case of the highest throughput fabrication was $N_p \simeq 17$ for the spot size $2w_0 = 1.22\lambda/NA$, $NA = 1.25$, $\lambda = 515$ nm and scan velocity of v_s = 6 mm/s. At the repetition rate $f_r = 75$ MHz and short laser pulses of $\tau_p = 20$ fs just a fs-oscillator is required to fabricate at the required irradiance and scanning velocities can be large making this a practical solution for applications. Indeed, for the same wavelength and focusing conditions, only $E_p = 0.1$ nJ is required for $I_p \simeq 2.5$ TW/cm^2. When thermal accumulation is present, i.e., a temperature diffusion time over the spot size, $2w_0$, is larger than the temporal separation between pulses, $1/f_r$, at typically $f_r \geq 0.5$ MHz in glasses and polymers [40], the thermally driven polymerization becomes possible. However, energy delivery should be very precisely controlled to avoid a thermal run away breakdown of an inherently exothermic polymerization reaction.

In order to increase the fabrication throughput, dry objective lenses should be used since approximately at $v_s > 1$ mm/s strong vibrations are introduced when immersion oil is mediating the objective lens contact with sample; this might be one of the reasons of the lower quality structures at the high velocities as recognizable in Fig. 7. High repetition fs-oscillators with short pulse duration of $\tau_p = 20$ fs can prove beneficial to further improve the demonstrated throughput values. Since short fs-pulses are sensitive to chirp in dispersive media, the ionization rate at the focus can be additionally controlled by controlling the chirp of the pulse [43]. Also, a spatial chirp - the pulse front tilt - can be used to control polymerization as it was demonstrated for the dielectric breakdown [44]. Combination of linear stage scan together with galvano scan in opposite directions would sum up the scanning velocities. The current state-of-the-art hardware typically used in fs-laser fabrication can deliver 10 cm/s speeds of the irradiation point on the samples's surface. This technique can become attractive for medical applications, e.g.,

#187315 - $15.00 USD Received 18 Mar 2013; revised 24 May 2013; accepted 30 May 2013; published 10 Jul 2013

fabrication of complex 3D networks of blood vessels [12, 45]. By combination of linear and galvano scanners, it is possible to reach 720 μm^3/s throughput using laser setup No. 1 with $NA \sim 1.25$ focusing. Hence, a high spatial resolution of structuring and almost 300$^\times$ higher throughput is achieved as compared to the current state-of-the-art in laser structuring of PDMS.

4. Conclusion

We have shown direct laser writing of 2D and 3D structures in PDMS elastomer with throughput of ~ 720 μm^3/s which is larger than that (~ 12 μm^3/s) reported previously [9, 10]. Structuring with visible 515 nm wavelength, 300 fs pulses at 200 kHz and $NA = 1.25$ focusing, the achieved throughput was ~ 720 μm^3/s while at the near-IR wavelength of 800 nm, 20 fs, 75 MHz and $NA = 1.4$ the throughput was ~ 20 μm^3/s.

Photo-initiators ISO and THIO at 0.2-1% wt were required for the high fidelity fabrication in viscous liquid PDMS photo-polymer. These photo-initiators are not toxic and fabricated structures can be used for cell cultures [46]. The 3D sculpturing at similar sample translation velocities with comparable average laser power were used in pure PDMS and with 0.2% wt THIO. Combination of stage and galvano-scanners allowed to achieve ~ 6 mm/s fabrication velocities and is promising for the high-throughput applications such as fabrication of bio-scaffolds. Apparently, use of scanners was beneficial to create smoother surfaces of fabricated structures.

Laser structuring employing avalanche ionization and thermal polymerization opens opportunity to create 3D structures out of pure biocompatible materials with 0% of photo-initiator. This does not change biological nor optical properties of materials already widely used in bio- and medical industries and mitigates aging problems related to dye-doping of polymers. Direct 3D sculpturing for the maskless manufacturing of molds used in soft-lithography or for the 3D components in microfluidic and optofluidic applications.

Acknowledgments

SR is grateful for support by FASTQUAST (PITN-GA-2008-214962) EU mobility grant and "BIOMATRIX" grant (No. 31V-43/2013) from the Agency for Science, Innovation and Technology. MM acknowledges financial support by MIKROŠVIESA research grant (No. MIP-12241) from the Research Council of Lithuania. SJ is grateful for partial support via Discovery grant DP120102980 from Australian Research Council. Authors would like to thank Dr. Maria Farsari for providing access to NonLinear Lithography laboratory (IESL-FORTH) and critical discussions; we thank Mrs. Aleka Manousaki for expert technical assistance with SEM.

#187315 - $15.00 USD Received 18 Mar 2013; revised 24 May 2013; accepted 30 May 2013; published 10 Jul 2013